LA-UR-84-4008

CONF-841259--1

Los Alamos National Laboratory is operated by the University of California for the United States Department of Energy under contract W-7405-ENG-36

LA-UR--84-4008

DE85 005580

TITLE: DYNAMICAL CALCULATIONS OF NUCLEAR FISSION AND HEAVY-ION REACTIONS

AUTHOR(S): J. Rayford Nix and Arnold J. Sierk

SUBMITTED TO: For presentation at the International Conference on Nuclear Physics, Bombay, India, December 27-31, 1984

Los Alamos National Laboratory
Los Alamos, New Mexico 87545

DYNAMICAL CALCULATIONS OF NUCLEAR FISSION AND HEAVY-ION REACTIONS

J. Rayford Nix and Arnold J. Sierk
Theoretical Division, Los Alamos National Laboratory
Los Alamos, New Mexico 87545, USA

ABSTRACT

With the goal of determining the magnitude and mechanism of nuclear dissipation from comparisons of predictions with experimental data, we describe recent calculations in a unified macroscopic-microscopic approach to large-amplitude collective nuclear motion such as occurs in fission and heavy-ion reactions. We describe the time dependence of the distribution function in phase space of collective coordinates and momenta by a generalized Fokker-Planck equation. The nuclear potential energy of deformation is calculated as the sum of repulsive Coulomb and centrifugal energies and an attractive Yukawa-plus-exponential potential, the inertia tensor is calculated for a superposition of rigid-body rotation and incompressible, nearly irrotational flow by use of the Werner-Wheeler method, and the dissipation tensor that describes the conversion of collective energy into single-particle excitation energy is calculated for two prototype mechanisms that represent opposite extremes of large and small dissipation. We solve the generalized Hamilton equations of motion for the first moments of the distribution function to obtain the mean translational fission-fragment kinetic energy and mass of a third fragment that sometimes forms between the two end fragments, as well as dynamical thresholds, capture cross sections, and ternary events in heavy-ion reactions.

1. INTRODUCTION

Nuclear physicists have been struggling for years to determine the magnitude and mechanism of nuclear dissipation--to answer two elementary questions: Is a nucleus overdamped like a drop of honey, or underdamped like a drop of water? Does a nucleus dissipate its energy of collective motion primarily through interactions of nucleons with the mean field generated by the remaining nucleons, or do two-particle collisions play a substantial role? Despite numerous experimental clues provided by fission and heavy-ion reactions, the answers to such questions posed by this challenging many-body problem have proved elusive. This is because of the many complementary aspects displayed by the atomic nucleus. With its relatively small number of degrees of freedom, the nucleus is both microscopic and macroscopic on the one hand and both quantal and classical on the other, which gives it a rich dynamical behaviour ranging from elastic vibrations of solids to long-mean-free-path dissipative fluid flow with statistical fluctuations. On this occasion of the Golden Jubilee of the Indian National Science Academy, we would like to tell you about some of our recent calculations at Los Alamos directed toward answering these questions.

Our approach is *not* to explain the experimental data in terms of some model with adjustable parameters--since often several models with widely different physical bases are capable of doing this equally well--but instead to find and calculate physical observables that depend sensitively upon the magnitude and mechanism of nuclear dissipation. The difficulty arises because many of the gross experimental features of fission and heavy-ion reactions are determined primarily by a competition between the attractive nuclear force and the repulsive Coulomb and centrifugal forces, and any theoretical approach that includes correctly these relatively trivial forces reproduces the data with fair accuracy. Also, the final effects on observable quantities caused by dissipation are often very similar to the final effects caused by collective degrees of freedom.

In our studies here, we consider two prototype mechanisms that represent opposite extremes of large and small dissipation. For these

two mechanisms we use a macroscopic-microscopic method to calculate observable quantities in fission and heavy-ion reactions and confront these predictions with experimental data in an attempt to determine the magnitude and mechanism of nuclear dissipation.

2. MACROSCOPIC-MICROSCOPIC METHOD

We focus from the outset on those few collective coordinates that are most relevant to the phenomena under consideration. In particular, for a system of A nucleons, we separate the 3A degrees of freedom representing their center-of-mass motion into N collective degrees of freedom that are treated explicitly and 3A - N internal degrees of freedom that are treated implicitly.

2.1 Collective Coordinates

In our earlier dynamical studies we have usually described the nuclear shape in terms of smoothly joined portions of three quadratic surfaces of revolution, with three symmetric and two independent asymmetric shape coordinates.[1-5] Although suitable for many purposes, this three-quadratic-surface parametrization breaks down in the later stages of many heavy-ion fusion calculations, is unable to describe division into more than two fragments, and leads to very complicated expressions for the forces involved.

Because of these disadvantages, we have switched[6] to a more suitable parametrization in which an axially symmetric nuclear shape is described in cylindrical coordinates by means of the Legendre-polynomial expansion[7]

$$\rho_s^2(z) = R_0^2 \sum_{n=0}^{N} q_n P_n[(z-\bar{z})/z_0] \quad . \tag{1}$$

In this expression, z is the coordinate along the symmetry axis, ρ_s is the value on the surface of the coordinate perpendicular to the symmetry axis, z_0 is one-half the distance between the two ends of the shape, $\bar{z}$ is the value of z at the midpoint between the two ends, R_0 is the radius of the spherical nucleus, P_n is a Legendre polynomial of degree n, and q_n for $n \neq 0$ and 1 are N - 1 shape coordinates. Since

the nucleus is assumed to be incompressible, the quantity q_0 is not independent but is instead determined by volume conservation. Also, q_1 is determined by fixing the center of mass. In addition, we include an angular coordinate $\theta \equiv q_{N+1}$ to describe the rotation of the nuclear symmetry axis in the reaction plane, which leads to a total of N collective coordinates $q = q_2,\ldots,q_{N+1}$ that are considered. Throughout this paper we use N = 11, corresponding to five independent symmetric and five independent asymmetric shape coordinates and one angular coordinate.

2.2 Potential Energy

We consider excitation energies that are sufficiently high that single-particle effects may be neglected and calculate the potential energy of deformation V(q) as the sum of repulsive Coulomb and centrifugal energies and an attractive Yukawa-plus-exponential potential,[8] with constants determined in a recent nuclear mass formula.[9] This generalized surface energy takes into account the reduction in energy arising from the nonzero range of the nuclear force in such a way that saturation is ensured when two semi-infinite slabs are brought into contact.

2.3 Kinetic Energy

The collective kinetic energy is given by

$$T = \frac{1}{2} M_{ij}(q)\, \dot{q}_i\, \dot{q}_j = \frac{1}{2} [M(q)^{-1}]_{ij}\, p_i\, p_j \quad , \tag{2}$$

where the collective momenta p are related to the collective velocities $\dot{q}$ by

$$p_i = M_{ij}(q)\, \dot{q}_j \quad . \tag{3}$$

In these equations and the remainder of this paper we use the convention that repeated indices are to be summed over from 2 to N + 1. At the high excitation energies and large deformations considered here, where pairing correlations have disappeared and near crossings of single-particle levels have become less frequent, the rotational moment of inertia is close to the rigid-body value[10] and the vibrational inertia is close to the incompressible, irrotational value.[11] We

therefore calculate the inertia tensor M(q), which is a function of the shape of the system, for a superposition of rigid-body rotation and incompressible, nearly irrotational flow. For this purpose we use the Werner-Wheeler method, which determines the flow in terms of circular layers of fluid.[1-6]

2.4 Dissipation Mechanisms

The coupling between the collective and internal degrees of freedom gives rise to a dissipative force whose mean component in the i-th direction may be written as

$$F_i = - \eta_{ij}(q)\, \dot{q}_j = - \eta_{ij}(q)\, [M(q)^{-1}]_{jk}\, p_k \quad . \tag{4}$$

For the calculation of the shape-dependent dissipation tensor $\eta(q)$ that describes the conversion of collective energy into single-particle excitation energy, we consider two prototype mechanisms that represent opposite extremes of large and small dissipation. The first mechanism is one-body dissipation,[4-6,12-15] which arises from collisions of nucleons with the moving nuclear surface and when the neck is smaller than a critical size also from the transfer of nucleons through it, with a magnitude that is completely specified by the model. The second mechanism is two-body viscosity,[2,4-6] which is responsible for dissipation in ordinary fluids. Because in nuclei the nucleon mean free path is long compared to the nuclear radius, the conventional result for this mechanism is not expected to apply. Nevertheless, with a coefficient of two-body viscosity that is adjusted to reproduce experimental results, it represents a tractable and useful phenomenological approach for describing small dissipation.

Compared to most of our previous calculations with one-body dissipation,[4,5,12] our present calculations incorporate three improvements. First, to describe the transition from the wall formula that applies to mononuclear shapes to the wall-and-window formula that applies to dinuclear shapes we now use the smooth interpolation[6]

$$\eta = \sin^2(\tfrac{\pi}{2}\alpha)\, \eta_{\text{wall}} + \cos^2(\tfrac{\pi}{2}\alpha)\, \eta_{\text{wall-and-window}} \quad , \tag{5}$$

where

$$\alpha = (r_{neck}/R_{min})^2 \tag{6}$$

is the square of the ratio of the neck radius r_{neck} to the transverse semi-axis R_{min} of the end fragment with the smaller value. Second, in determining the drift velocities of the end fragments relative to which velocities in the wall-and-window formula are measured, we now require the conservation of linear and angular momentum rather than using the velocities of the centers of mass.[6] However, the results calculated with both prescriptions for the drift velocity are nearly identical. Third, for asymmetric shapes we now also take into account the dissipation associated with a time rate of change of the mass asymmetry degree of freedom in the completed wall-and-window formula.[14,15]

2.5 Generalized Fokker-Planck Equation

In addition to the mean dissipative force, the coupling between the collective and internal degrees of freedom gives rise to a residual fluctuating force, which we treat under the Markovian assumption that it does not depend upon the system's previous history. At high excitation energies, where classical statistical mechanics is valid, we are led to the generalized Fokker-Planck equation

$$\frac{\partial f}{\partial t} + (M^{-1})_{ij}\, p_j \frac{\partial f}{\partial q_i} - \left[\frac{\partial V}{\partial q_i} + \frac{1}{2}\frac{\partial (M^{-1})_{jk}}{\partial q_i}\, p_j\, p_k\right]\frac{\partial f}{\partial p_i}$$

$$= \eta_{ij}\,(M^{-1})_{jk}\frac{\partial}{\partial p_i}(p_k f) + \tau\eta_{ij}\frac{\partial^2 f}{\partial p_i \partial p_j} \tag{7}$$

for the dependence upon time t of the distribution function f(q,p,t) in phase space of collective coordinates and momenta. The last term on the right-hand side of this equation describes the spreading of the distribution function in phase space, with a rate that is proportional to the dissipation strength and the nuclear temperature τ, which is measured here in energy units.

2.6 Generalized Hamilton Equations

Although a useful approximate solution of a two-dimensional

Fokker-Planck equation has been obtained recently,[16] it is still difficult in practice to solve the generalized Fokker-Planck equation except for special cases. Therefore, in some of our studies we use equations for the time rate of change of the first moments of the distribution function, with the neglect of higher moments. These are the generalized Hamilton equations

$$\dot{q}_i = (M^{-1})_{ij}\, p_j \tag{8}$$

and

$$\dot{p}_i = -\frac{\partial V}{\partial q_i} - \frac{1}{2}\frac{\partial (M^{-1})_{jk}}{\partial q_i}\, p_j\, p_k - \eta_{ij}\,(M^{-1})_{jk}\, p_k \quad , \tag{9}$$

which we solve numerically for each of the N generalized coordinates and momenta.

3. FISSION

As our first application, we calculate for the fission of nuclei throughout the periodic table their mean translational fission-fragment kinetic energies and compare with experimental values. Although similar to earlier studies,[2,4] our present calculations are performed, as discussed above, with a more flexible shape parametrization, with a more realistic set of constants, and with an improved treatment of one-body dissipation. Also, our initial conditions at the fission saddle point now incorporate the effect of dissipation on the fission direction[17] and are calculated for excited nuclei with nuclear temperature $\tau = 2$ MeV by determining the mean velocity of all nuclei that pass per unit time through the saddle point with positive velocity.[18] Because this procedure is no longer valid when the fission barrier is less than the nuclear temperature, in such cases we use the mean velocity of the nucleus whose barrier is 2 MeV high. The atomic number Z is related to the mass number A according to Green's approximation to the valley of beta stability.[19] Our calculations for two-body viscosity are performed with viscosity coefficient

$$\mu = 0.02\ TP = 1.25 \times 10^{-23}\ \text{MeV s/fm}^3 \quad , \tag{10}$$

which as we see later is the value required to optimally reproduce experimental mean fission-fragment kinetic energies.

3.1 Dynamical Descent

In our fission calculations we specialize to reflection-symmetric shapes and zero angular momentum, so that only five coordinates are considered explicitly. The mean dynamical trajectories in deformation space for light nuclei correspond to short descents from dumbbell-like saddle-point shapes to compact scission shapes, whereas those for heavy nuclei correspond to long descents from cylinder-like saddle-point shapes to elongated scission shapes. Compared to the trajectories for nonviscous nuclei, those for one-body dissipation lead to more elongated scission shapes for light nuclei and to more compact scission shapes for heavy nuclei. In contrast, the trajectories for two-body viscosity always lead to more elongated scission shapes.

3.2 Ternary Division

An exciting new aspect of these dynamical calculations is the formation of a third fragment between the two end fragments for sufficiently heavy nuclei with either no dissipation or small two-body viscosity. As shown in Fig. 1, the mass of this third fragment increases with increasing $Z^2/A^{1/3}$ above a critical value that is slightly lower for two-body viscosity than for no dissipation. Since no third fragment is formed with one-body dissipation, accurate experimental information concerning such true ternary-fission processes should help decide the nuclear-dissipation issue. Further theoretical aspects of this problem are currently being studied at Los Alamos by Cârjan.[20]

3.3 Fission-Fragment Kinetic Energies

In calculating the mean fission-fragment translational kinetic energy at infinity, we treat the post-scission dynamical motion in terms of two spheroids, with initial conditions determined by keeping continuous the values of two moments and their time derivatives. When a small third fragment is formed in a realistic situation off the

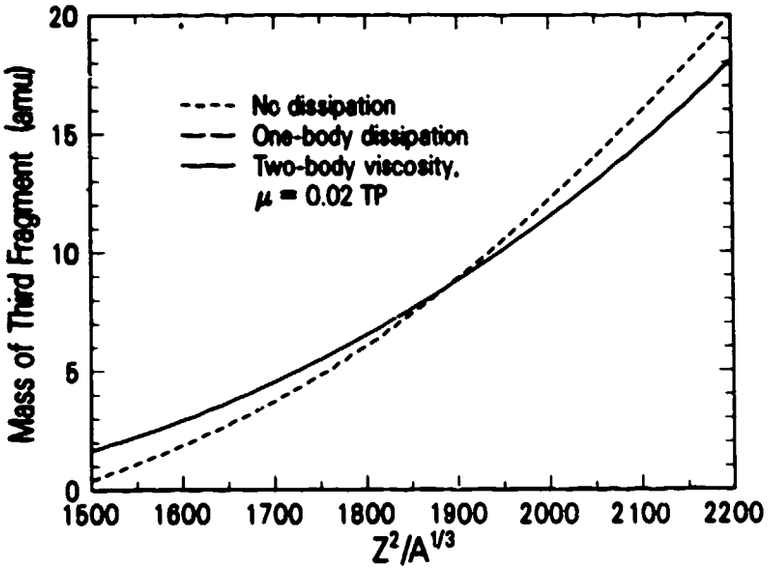

Figure 1
Effect of dissipation on the formation of a third fragment between the two end fragments.

symmetry axis and/or with some transverse velocity, it moves away and contr butes less to the kinetic energy of the two larger end fragments than it would in our idealized calculation, where it remains stationary at its origin. In the presence of a third fragment, we obtain a lower limit to the fission-fragment kinetic energy by calculating the post-scission separation of the end fragments in the absence of the middle fragment. Also, we estimate an upper limit in terms of the kinetic energy at scission of the two end fragments plus the Coulomb interaction energy of three spherical nuclei positioned at their respective centers of charge.

As the nucleus descends dynamically from its fission saddle point, the repulsive Coulomb force can overcome the attractive nuclear force and rupture the neck prior to its reaching a zero radius, as is required in our calculations. Although such a neck rupture at a nonzero radius would increase the calculated kinetic energy slightly,[21] we neglect this effect here because of the difficulty of properly incorporating the nuclear compressibility energy, which plays a crucial role in the neck-rupture process.

We compare in Figs. 2 and 3 our mean kinetic energies calculated in this way with experimental values for the fission of nuclei at high excitation energy,[2,22,23] where single-particle effects have decreased in importance. As shown by the short-dashed curves in both figures, the results calculated with no dissipation are for heavy nuclei substantially higher than the experimental values. Dissipation of either type lowers the calculated kinetic energy. However, as shown by the long-dashed curve in Fig. 2, one-body dissipation with a magnitude that is specified by the theory predicts for heavy nuclei values that lie below the experimental data. This underprediction arises because the highly dissipative descent from the saddle point damps out much of the pre-scission kinetic energy, and our improved parametrization leads to moderately elongated scission shapes with lower Coulomb repulsion. We regard this discrepancy as experimentally

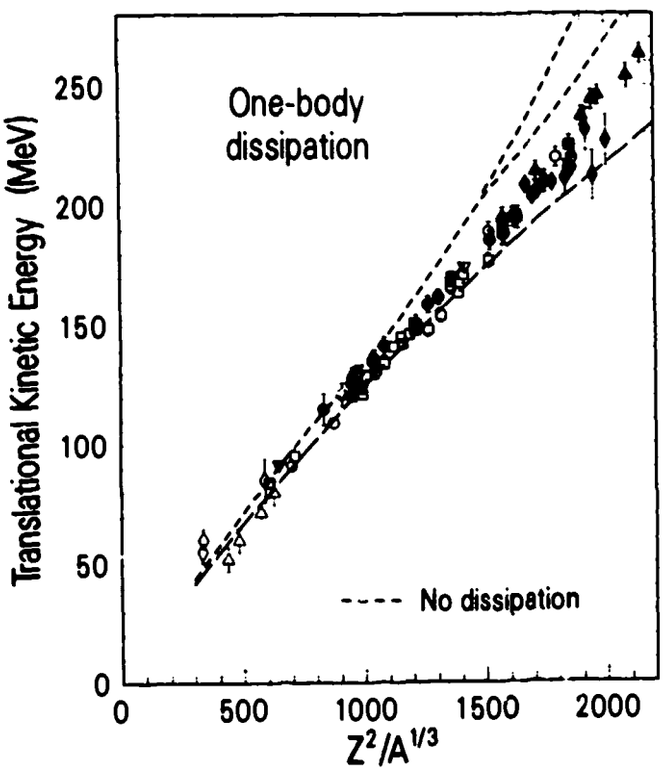

Figure 2
Reduction of mean fission-fragment kinetic energies by one-body dissipation, compared to experimental values.

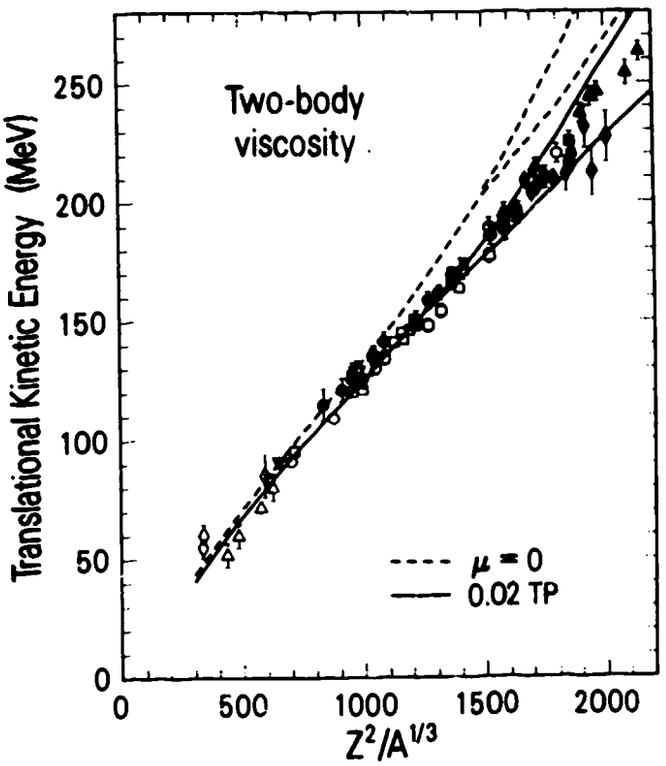

Figure 3
Reduction of mean fission-fragment kinetic energies by two-body viscosity, compared to experimental values.

demonstrating that one-body dissipation as presently formulated is *not* the complete dissipation mechanism in large-amplitude collective nuclear motion.

In contrast, as shown by the solid curves in Fig. 3, when the two-body viscosity coefficient is adjusted to the value μ = 0.02 TP, the experimental data for heavy nuclei lie between the calculated lower and upper limits and are adequately reproduced throughout the rest of the periodic table. For two-body viscosity, the dynamical trajectories lead to elongated scission shapes with less Coulomb repulsion, but this is supplemented by some pre-scission kinetic energy. These results calculated with several improvements demonstrate that mean fission-fragment kinetic energies are capable after all of distinguishing between dissipation mechanisms.

4. HEAVY-ION REACTIONS

Even better prospects for determing the dissipation mechanism reside with heavy-ion reactions, where we are able to choose the total mass of the combined system, the mass asymmetry of the entrance channel, and the bombarding energy with foresight. This permits us to select for study those dynamically interesting cases that involve large distances in deformation space.

4.1 Dynamical Thresholds for Fusion

A necessary condition for compound-nucleus formation is that the dynamical trajectory of the fusing system pass inside the fission saddle point in a multidimensional deformation space. For heavy nuclear systems and/or large impact parameters, the fission saddle point lies inside the contact point, and the center-of-mass bombarding energy must exceed the maximum in the one-dimensional zero-angular-momentum interaction barrier by an amount ΔE in order to form a compound nucleus.

This additional energy ΔE has been calculated for symmetric nuclear systems both by solving the generalized Hamilton equations numerically with the three-quadratic-surface shape parametrization and realistic forces[3,5,6] and approximately with the two-sphere-plus-conical-neck shape parametrization and schematic forces.[14,24,25] Such values calculated for symmetric nuclear systems have been compared with experimental values derived from asymmetric nuclear systems under various assumptions concerning the scaling of asymmetric systems into symmetric ones.[5,6,14,23-28] However, our recent calculations involving asymmetric systems indicate that none of the scaling assumptions are sufficiently accurate for detailed comparisons.

We therefore compare here our values of the additional energy ΔE calculated for five specific nuclear systems for which neutron-evaporation-residue cross sections have been recently measured[28,29] and analyzed to yield experimental thresholds.[28] As indicated in Table 1, as we progress through these systems the additional energy calculated with two-body viscosity increases from less than 1 MeV, representing only the energy that is dissipated during the approach stage,

Table 1

Comparison of calculated and experimental values of the additional energy ΔE required to form a compound nucleus, measured relative to the maximum in the calculated one-dimensional zero-angular-momentum interaction barrier. The calculated values of additional energy are for two-body viscosity with coefficient $\mu = 0.02$ TP.

Reaction	Calculated one-dimensional barrier (MeV)	Calculated additional energy (MeV)	Experimental additional energy (MeV)	Note
$^{90}Zr + {}^{90}Zr \rightarrow {}^{180}Hg$	189.0	0.9	-7 ± 2	a
$^{86}Kr + {}^{123}Sb \rightarrow {}^{209}Fr$	209.0	0.9	0^{+4}_{-2}	
$^{124}Sn + {}^{96}Zr \rightarrow {}^{220}Th$	224.7	1.2	16^{+5}_{-3}	b
$^{124}Sn + {}^{94}Zr \rightarrow {}^{218}Th$	225.5	6.5	13^{+5}_{-3}	c
$^{124}Sn + {}^{92}Zr \rightarrow {}^{216}Th$	226.3	8.2	11^{+4}_{-3}	

[a]For this reaction involving nuclei lighter than those requiring an additional energy, the negative experimental value of ΔE suggests the importance of zero-point vibrations on the low-energy fusion cross section (Ref. 30).

[b]For this reaction involving a target for which the calculated value of Nilsson's spheroidal deformation coordinate $\varepsilon = 0.20$ (Refs. 9 and 31), the large experimental value of ΔE compared to the calculated value suggests the importance of static ground-state deformations on the additional energy.

[c]For this reaction involving a target for which the calculated value of Nilsson's spheroidal deformation coordinate $\varepsilon = -0.12$ (Refs. 9 and 31), the moderately large experimental value of ΔE compared to the calculated value suggests the importance of static ground-state deformations on the additional energy.

to several MeV, representing in addition the energy required to dynamically push the system inside its fission saddle point. The experimental values show a similar trend, but three large deviations from the calculated values suggest the important role played by zero-point vibrations and static ground-state deformations, as discussed in the footnotes to Table 1. Our analogous calculations with one-body

dissipation are not yet completed; like the rest of you at this Conference, we are eagerly awaiting their outcome.

4.2 Capture Cross Section

For the reaction $^{208}Pb + ^{58}Fe$ that has been studied experimentally by Bock et al.,[26] we calculate the capture cross section corresponding to the transfer of 40 or more nucleons from the heavier ^{208}Pb nucleus to the lighter ^{58}Fe nucleus. Our calculated results are compared in Fig. 4 with experimental values resulting from a revised analysis in which the experimental capture cross section is defined in terms of reaction products with fully relaxed total kinetic energy and masses lying between the deep-inelastic peaks.[23] The cross section calculated with two-body viscosity is somewhat larger than the experimental points at all energies except near the threshold.

We have not yet finished our analogous calculations with one-body dissipation when the additional term in the completed wall-and-window formula is included because it requires the specification of a mass asymmetry, which is difficult for shapes with long necks. When this

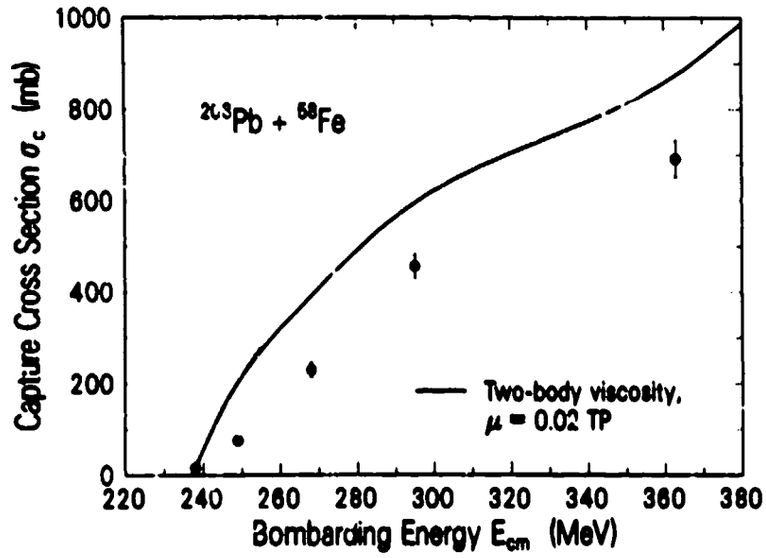

Figure 4
Capture cross section calculated with two-body viscosity, compared to revised experimental values (Ref. 23).

additional term is omitted, the capture cross section calculated with one-body dissipation is even larger at intermediate and high energies than that calculated with two-body viscosity, but the additional term is expected to reduce it. Similar calculations with a restricted shape parametrization where the present difficulties did not arise have been performed by Błocki,[32] who adjusted his interpolation procedure to reproduce the original *unrevised* experimental data for a comparable reaction.[26]

4.3 Ternary Events

We consider next the reaction $^{129}Xe + ^{122}Sn$ at a laboratory bombarding energy per nucleon of 12.5 MeV studied experimentally by Gläs-sel et al.,[33] for which ternary events were observed approximately 10% of the time when the energy loss was large. Glässel et al. deduced that the time between successive scission events is approximately 1×10^{-21} s, during which the two primary fragments move only a few nuclear radii apart and perform only a fraction of a rotation. The ratio of mean fragment masses for the second scission event was determined to be approximately 1.5.

Figures 5 and 6 show sequences of shapes calculated for this reaction for angular momentum $L = 250$ and 350 $\hbar$, respectively. In these two figures our results with one-body dissipation are calculated for computational ease without the additional term in the wall-and-window formula, which has little effect since the system is nearly symmetric. With this dissipation mechanism, the process is essentially binary, with only extremely small third fragments forming between the two end fragments. In contrast, two-body viscosity with coefficient $\mu = 0.02$ TP leads to true ternary events, with middle-fragment masses of 51.4 and 69.1 amu for $L = 250$ and 350 $\hbar$, respectively. The mass ratio of the forward-going fragment to the middle fragment is 1.93 for $L = 250\ \hbar$ and 1.32 for $L = 350\ \hbar$.

Although in our calculations with two-body viscosity, which refer to mean events, the two necks reach zero radius at essentially the same time, fluctuations could introduce some difference. Also, the scission-to-scission time of 1×10^{-21} s deduced by Glässel et al. was

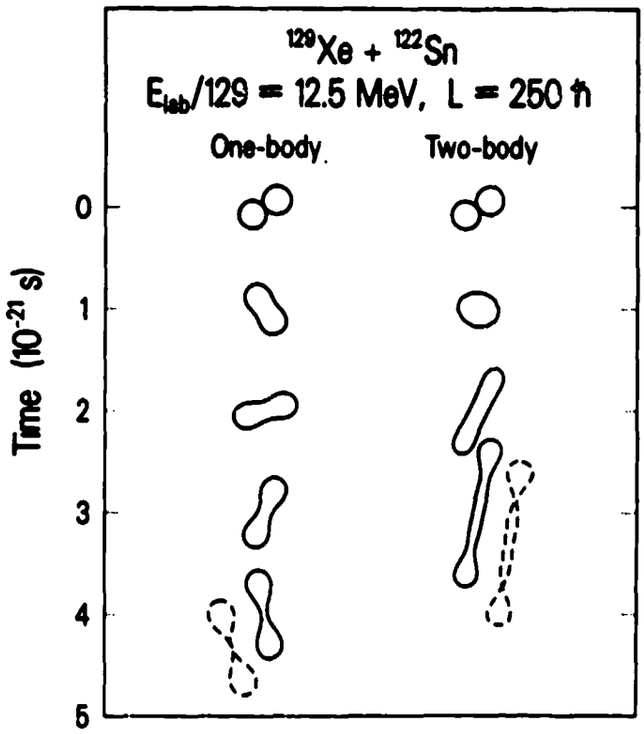

Figure 5
Effect of dissipation on ternary heavy-ion events for angular momentum $L = 250\,\hbar$. The ^{129}Xe projectile is incident from the right. For clarity, the dashed scission shapes are shown displaced from their proper horizontal positions.

based on certain assumptions concerning nuclear shapes that are very different from those calculated here. Although the probability for ternary events in our calculations with two-body viscosity is much larger than the approximately 10% observed by Glässel et al., the experimental arrangement could have missed events in which the middle fragment remained essentially at rest in the center-of-mass system and detected instead only those with some forward velocity resulting once again from fluctuations. Although several issues remain to be clarified, it is possible that the ternary events seen by Glässel et al. have a dynamical origin of the type calculated here for *small* two-body viscosity. If so, this could provide a convincing discrimination between the two extremes of dissipation that we are considering.

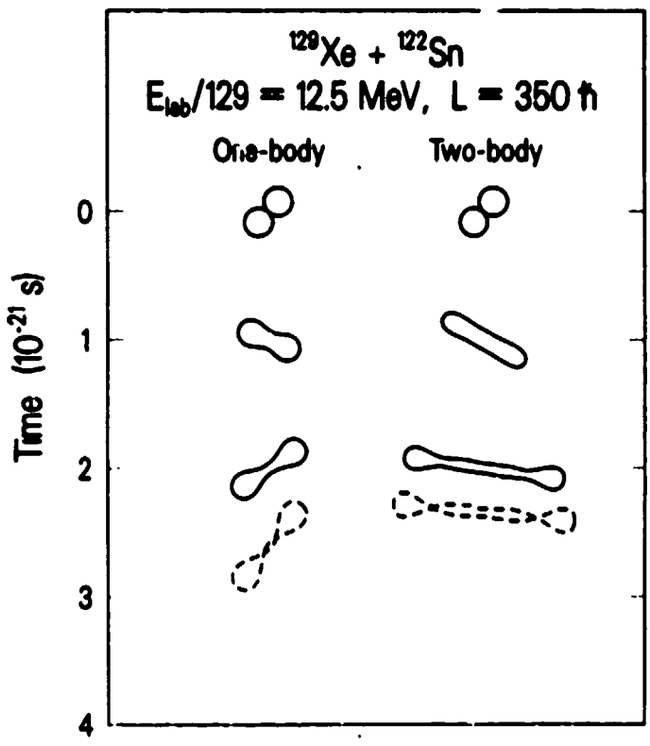

Figure 6
Effect of dissipation on ternary heavy-ion events for angular momentum $L = 350\ \hbar$. The ^{129}Xe projectile is incident from the right.

5. CONCLUSION

We are entering a new era in fission and heavy-ion reactions. Up to now theoretical approaches with vastly different pictures of the underlying nuclear dynamics have reproduced many of the gross experimental features of fission and heavy-ion reactions because they include correctly the dominant nuclear, Coulomb, and centrifugal forces. However, calculations are now being designed specifically to test the dissipation mechanism. When compared with mean fission-fragment kinetic energies, these calculations demonstrate that one-body dissipation is not the complete dissipation mechanism. The next step is to compute dynamical thresholds for fusion and capture cross sections with one-body dissipation and compare with experimental results.

Ternary heavy-ion events offer the most exciting prospect for finally determining the magnitude and mechanism of nuclear dissipa-

tion. If experimentally observed ternary events turn out to have a dynamical origin of the type calculated here with two-body viscosity, this would suggest small dissipation in nuclei. In this eventuality the theoretical challenge would be to understand the mechanism, since the long nucleon mean free path eliminates the conventional two-body mechanism that is present in ordinary fluids.

ACKNOWLEDGEMENTS

We are grateful to T. C. Awes, B. B. Back, S. Bjørnholm, N. Cârjan, A. Gavron, F. Plasil, J. Randrup, W. J. Swiatecki, R. Vandenbosch, and J. B. Wilhelmy for stimulating discussions. This work was supported by the U. S. Department of Energy.

REFERENCES

1. J. R. Nix, Nucl. Phys. A130, 241 (1969).
2. K. T. R. Davies, A. J. Sierk, and J. R. Nix, Phys. Rev. C13, 2385 (1976)
3. J. R. Nix and A. J. Sierk, Phys. Rev. C15, 2072 (1977).
4. A. J. Sierk and J. R. Nix, Phys. Rev. C21, 982 (1980).
5. K. T. R. Davies, A. J. Sierk, and J. R. Nix, Phys. Rev. C28, 679 (1983).
6. J. R. Nix and A. J. Sierk, Nucl. Phys. A428, 161c (1984).
7. S. Trentalange, S. E. Koonin, and A. J. Sierk, Phys. Rev. C22, 1159 (1980).
8. H. J. Krappe, J. R. Nix, and A. J. Sierk, Phys. Rev. C20, 992 (1979).
9. P. Möller and J. R. Nix, Nucl. Phys. A361, 117 (1981).
10. J. Kunz and U. Mosel, Nucl. Phys. A406, 269 (1983).
11. J. Kunz and J. R. Nix, Los Alamos National Laboratory Preprint LA-UR-84-2580 (1984).
12. J. Błocki, Y. Boneh, J. R. Nix, J. Randrup, M. Robel, A. J. Sierk, and W. J. Swiatecki, Ann. Phys. (N. Y.) 113, 330 (1978).
13. J. Randrup and W. J. Swiatecki, Ann. Phys. (N. Y.) 125, 193 (1980).
14. W. J. Swiatecki, Nucl. Phys. A428, 199c (1984).
15. J. Randrup and W. J. Swiatecki, Nucl. Phys. A429, 105 (1984).

16. F. Scheuter, C. Grégoire, H. Hofmann, and J. R. Nix, Grand Accélérateur National d'Ions Lourds Preprint GANIL-P.84.09 (1984).

17. K. T. R. Davies, J. R. Nix, and A. J. Sierk, Phys. Rev. C28, 1181 (1983).

18. J. R. Nix, A. J. Sierk, H. Hofmann, F. Scheuter, and D. Vautherin, Nucl. Phys. A424, 239 (1984).

19. A. E. S. Green, *Nuclear Physics* (McGraw-Hill, New York, 1955), pp. 185, 250.

20. N. Cârjan, private communication.

21. K. T. R. Davies, R. A. Managan, J. R. Nix, and A. J. Sierk, Phys. Rev. C16, 1890 (1977).

22. D. v. Harrach, P. Glässel, Y. Civelekoğlu, R. Männer, H. J. Specht, J. B. Wilhelmy, H. Freiesleben, and K. D. Hildebrand, in *Proc. Int. Symp. on Physics and Chemistry of Fission, Jülich, 1979* (International Atomic Energy Agency, Vienna, 1980), p. 575.

23. J. Töke, R. Bock, G. X. Dai, S. Gralla, A. Gobbi, K. D. Hildenbrand, J. Kuzminski, W. F. J. Müller, A. Olmi, H. Stelzer, B. B. Back, and S. Bjørnholm, Gesellschaft für Schwerionenforschung Preprint GSI-84-51 (1984).

24. W. J. Swiatecki, Phys. Scr. 24, 113 (1981).

25. S. Bjørnholm and W. J. Swiatecki, Nucl. Phys. A391, 471 (1982).

26. R. Bock, Y. T. Chu, M. Dakowski, A. Gobbi, E. Grosse, A. Olmi, H. Sann, D. Schwalm, U. Lynen, W. Müller, S. Bjørnholm, H. Esbensen, W. Wölfli, and E. Morenzoni, Nucl. Phys. A388, 334 (1982).

27. R. Vandenbosch, University of Washington Preprint (1984).

28. C. C. Sahm, H. G. Clerc, K. H. Schmidt, W. Reisdorf, P. Armbruster, F. P. Hessberger, J. G. Keller, G. Münzenberg, and D. Vermeulen, Technische Hochschule Darmstadt Preprint (1984).

29. J. G. Keller, K. H. Schmidt, H. Stelzer, W. Reisdorf, Y. K. Agarwal, F. P. Hessberger, G. Münzenberg, H. G. Clerc, and C. C. Sahm, Phys. Rev. C29, 1569 (1984).

30. T. Kodama, R. A. M. S. Nazareth, P. Möller, and J. R. Nix, Phys. Ref. C17, 111 (1978).

31. P. Möller and J. R. Nix, Atomic Data Nucl. Data Tables 26, 165 (1981).

32. J. Błocki, J. Phys. (Paris) 45, C6-489 (1984).

33. P. Glässel, D. v. Harrach, H. J. Specht, and L. Grodzins, Z. Phys. A310, 189 (1983).